

Mathematical Construction of a Reissner-Mindlin Plate Theory for Composite Laminates*

Wenbin Yu[†]

Utah State University, Logan, Utah 84322-4130

A Reissner-Mindlin theory for composite laminates without invoking *ad hoc* kinematic assumptions is constructed using the variational-asymptotic method. Instead of assuming *a priori* the distribution of three-dimensional displacements in terms of two-dimensional plate displacements as what is usually done in typical plate theories, an exact intrinsic formulation has been achieved by introducing unknown three-dimensional warping functions. Then the variational-asymptotic method is applied to systematically decouple the original three-dimensional problem into a one-dimensional through-the-thickness analysis and a two-dimensional plate analysis. The resulting theory is an equivalent single-layer Reissner-Mindlin theory with an excellent accuracy comparable to that of higher-order, layerwise theories. The present work is extended from the previous theory developed by the writer and his co-workers with several sizable contributions: (a) six more constants (33 in total) are introduced to allow maximum freedom to transform the asymptotically correct energy into a Reissner-Mindlin model; (b) the semi-definite programming technique is used to seek the optimum Reissner-Mindlin model; Furthermore, it is proved the first time that the recovered three-dimensional quantities exactly satisfy the continuity conditions on the interface between different layers and traction boundary conditions on the bottom and top surfaces. It is also shown that two of the equilibrium equations of three-dimensional elasticity can be satisfied asymptotically, and the third one can be satisfied approximately so that the difference between the Reissner-Mindlin model and the second order asymptotical model can be minimized. Numerical examples are presented to compare with the exact solution as well as the classical lamination theory and the first-order shear-deformation theory, demonstrating that the present theory has an excellent agreement with the exact solution.

*A preliminary version of this paper appeared in the proceedings of 2004 ASME International Mechanical Engineering Congress and Exposition, Anaheim, California, Nov. 13 – 19, 2004.

[†]Assistant Professor, Department of Mechanical and Aerospace Engineering.

Introduction

Recent decades have seen many new theories on composite laminates in the literature accompanying the increased application of composite materials in practice. However, engineers are reluctant to accept them with confidence due to two main reasons: (1) most of the theories are constructed for specific problems without sufficient generalization (both the plate itself and various analyses associated with it) and (2) some models with sufficient accuracy are too complicated and computationally inefficient to be used for design purposes. Simple yet efficient, accurate, and generalized analysis tools are still in need to provide high-fidelity prediction, shorten the design period, and reduce the cost of composite structures.

Many structures made with composite materials have one dimension much smaller than the other two and can be modelled as plates. Composite plate models are generally derived from three-dimensional (3-D) anisotropic elasticity theory, making use of the thinness of the plate. The simplest composite plate theory is the classical lamination theory (CLT), which is based on the Kirchhoff hypothesis. It is well known, however, that composite plates do not have to be very thick in order for this theory to yield extremely poor results compared to the exact 3-D solution. Although it is plausible to take into account the smallness of the thickness of such structures, construction of an accurate two-dimensional (2-D) model for a 3-D body still introduces a lot of challenges. There have been many attempts to rationally improve upon CLT such as those reviewed in Noor and Burton (1989), Noor and Burton (1990), and Noor and Malik (2000)). Most of the models, for example Reddy (1984), Touratier (1991), DiSciuva (1985), and Cho and Averill (2000), are based on *ad hoc* kinematic assumptions, such as an *a priori* distribution of displacement through the thickness.

Mathematically, the approximation in the process of constructing a plate theory stems from elimination of the thickness coordinate from the independent variables of the governing equations, a dimensional reduction process. This sort of approximation is inevitable if one wants to take advantage of the smallness of the thickness to simplify the analysis. However, other approximations that are not absolutely necessary should be avoided. For example, for small-strain analysis of plates, it is reasonable to assume that the thickness, h , is small compared to the wavelength of deformation of the reference plane, l . However, it is unnecessary to assume *a priori* some *ad hoc* displacement field, although that is the way most plate theories are constructed.

Recently, a mathematical approach, variational asymptotic method (VAM) introduced by Berdichevsky (1979), has been adopted to construct accurate models for composite laminates (Yu *et al.* (2002), Yu *et al.* (2003), and Yu and Hodges (2004)). In this approach, we first cast the original 3-D elasticity problem in an intrinsic form so that the theory can accommodate arbitrarily large displacement and global rotation, subject only to the strain being small (see

Danielson (1991)). Then, VAM is employed to reduce the dimensionality systematically in terms of the smallness of h/l . VAM can rigorously split the original nonlinear 3-D elasticity problem into a linear, one-dimensional (1-D), through-the-thickness analysis and a nonlinear, 2-D, plate analysis. The through-the-thickness analysis produces a 2-D constitutive law to be used in the plate analysis, along with recovery relations that yield the 3-D displacement, strain, and stress fields using results obtained from the solution of the 2-D plate analysis.

To avoid the overwhelming complexity of the plate model constructed directly using asymptotic methods, one can transfer this model into a simple engineering model, such as the Reissner-Mindlin model. To minimize the loss of accuracy during the transformation, we should allow the maximum freedom to seek the optimal engineering model, which is achieved in this paper by introducing six more constants than the previous work in Yu *et al.* (2002). Another contribution of the present work is to use the semi-definite programming (see Toh *et al.* (1999)) technique to perform the optimization, which is more mathematically sound than the least squares technique for our present purpose. Moreover, it is proved the first time that the reduced model constructed this way automatically satisfies the continuity conditions, including both the displacements and stresses, on the interface between different layers and traction boundary conditions on the bottom and top surfaces. It is also shown that the first two of the equilibrium equations of 3-D elasticity can be satisfied asymptotically, and the third one can be satisfied approximately in a sense of minimal energy loss. Several numerical examples are presented to validate the present theory against available exact solutions and other approximate models.

Three-Dimensional Formulation

A point in the plate can be described by its Cartesian coordinates x_i (see Fig. 1), where x_α are two orthogonal lines in the reference plane and x_3 is the normal coordinate. (Here and throughout the paper, Greek indices assume values 1 and 2 while Latin indices assume 1, 2, and 3. Repeated indices are summed over their range except where explicitly indicated.) Letting \mathbf{b}_i denote the unit vector along x_i for the initial configuration, one can then describe the position of any material point in the plate by its position vector $\hat{\mathbf{r}}$ from a fixed point O

$$\hat{\mathbf{r}}(x_1, x_2, x_3) = \mathbf{r}(x_1, x_2) + x_3\mathbf{b}_3 \quad (1)$$

where \mathbf{r} is the position vector from O to the point located by x_α on the reference plane. If the mid-plane is chosen as the reference plane, we have

$$\langle \hat{\mathbf{r}}(x_1, x_2, x_3) \rangle = h\mathbf{r}(x_1, x_2) \quad (2)$$

where the angle-brackets denote the definite integral through the thickness of the plate and will be used throughout the paper.

When the plate deforms, the particle that had position vector $\hat{\mathbf{r}}$ in the undeformed state now has position vector $\hat{\mathbf{R}}$ in the deformed plate. The latter can be uniquely determined by the deformation of the 3-D body. We introduce another triad \mathbf{B}_i for the deformed configuration so that:

$$\mathbf{B}_i = C_{ij}\mathbf{b}_j \quad C_{ij} = \mathbf{B}_i \cdot \mathbf{b}_j \quad (3)$$

subject to the requirement that \mathbf{B}_i is coincident with \mathbf{b}_i when the structure is undeformed. The direction cosines matrix $C(x_1, x_2)$ represents the possible arbitrary rotation between \mathbf{B}_i and \mathbf{b}_i . Now, the position vector $\hat{\mathbf{R}}$ can be represented as

$$\hat{\mathbf{R}}(x_1, x_2, x_3) = \mathbf{R}(x_1, x_2) + x_3\mathbf{B}_3 + w_i(x_1, x_2, x_3)\mathbf{B}_i \quad (4)$$

where w_i are the warping functions of the normal-line element which are treated as unknown 3-D functions to be solved for later. To ensure a one-to-one mapping between $\hat{\mathbf{R}}$ and $(\mathbf{R}, \mathbf{B}_i, w_i)$, we need to introduce six constraints by choosing appropriate definitions of \mathbf{R} and \mathbf{B}_i . One can define \mathbf{R} as

$$h\mathbf{R} = \langle \hat{\mathbf{R}} \rangle - c_i \quad (5)$$

which means the warping functions satisfy the following constraints

$$\langle w_i(x_1, x_2, x_3) \rangle = c_i \quad (6)$$

where c_i are arbitrary functions of the in-plane coordinates x_α introduced for the convenience of construction of an optimal Reissner-Mindlin model.

We are free to choose \mathbf{B}_3 as the normal to the reference plane of the deformed plate to introduce additional two constraints. It should be noted that this is a convenient choice and has nothing to do with the Kirchhoff hypothesis. In the Kirchhoff hypothesis, no local deformation of the transverse normal is allowed. However, according to the present scheme we allow all possible deformation by (a) classifying all deformation other than that of classical plate theory as warping, (b) assuming that the strain is small, and (c) requiring that the relative rotation of a differential element of the transverse normal caused by warping is of the order of the strain.

Another constraint is introduced by rotating the set of \mathbf{B}_α such that

$$\mathbf{B}_1 \cdot \mathbf{R}_{,2} = \mathbf{B}_2 \cdot \mathbf{R}_{,1} \quad (7)$$

So far, a total of six constraints have been introduced. The arbitrariness of c_i means there is a family of asymptotical theories. These constants will be determined by seeking the “best” Reissner-Mindlin model from the above family so that the loss of accuracy is minimized. Once c_i are determined, the warping functions will be uniquely determined and the 3-D variables will be uniquely expressed in terms of the 2-D variables and warping functions as shown in Eq. (4).

Based on the concept of decomposition of rotation tensor, Danielson (1991), the 3-D strains for small local rotation are

$$\Gamma_{ij} = \frac{1}{2}(F_{ij} + F_{ji}) - \delta_{ij} \quad (8)$$

where F_{ij} are the mixed-basis components of the deformation gradient tensor such that

$$F_{ij} = \mathbf{B}_i \cdot \mathbf{G}_k \mathbf{g}^k \cdot \mathbf{b}_j \quad (9)$$

with \mathbf{G}_k as the covariant basis vector of the deformed configuration and \mathbf{g}^k the contravariant base vector of the undeformed configuration. It is obvious that $\mathbf{g}^k = \mathbf{g}_k = \mathbf{b}_k$. One can obtain \mathbf{G}_k with the help of the definition of so-called generalized 2-D strains (see Hodges *et al.* (1993)), given by

$$\mathbf{R}_{,\alpha} = \mathbf{B}_\alpha + \varepsilon_{\alpha\beta} \mathbf{B}_\beta \quad (10)$$

$$\mathbf{B}_{i,\alpha} = (-K_{\alpha\beta} \mathbf{B}_\beta \times \mathbf{B}_3 + K_{\alpha 3} \mathbf{B}_3) \times \mathbf{B}_i \quad (11)$$

where $\varepsilon_{\alpha\beta}$ and $K_{\alpha\beta}$ are the 2-D generalized strains and $(\cdot)_{,\alpha} = \frac{\partial(\cdot)}{\partial x_\alpha}$. From Eq. (10), one can find out that the meaning of the sixth constraint in Eq. (7) is to choose $\varepsilon_{12} = \varepsilon_{21}$.

With the assumption that the strain is small compared to unity, which has the effect of removing all the terms that are products of the warping and the generalized strains, one can express the 3-D strain field as

$$\begin{aligned} \Gamma_e &= \epsilon + x_3 \kappa + I_1 w_{\parallel,1} + I_2 w_{\parallel,2} \\ 2\Gamma_s &= w'_{\parallel} + e_1 w_{3,1} + e_2 w_{3,2} \\ \Gamma_t &= w'_3 \end{aligned} \quad (12)$$

where $(\cdot)' = \frac{\partial(\cdot)}{\partial x_3}$, $(\cdot)_{\parallel} = [(\cdot)_1 \ (\cdot)_2]^T$ and

$$\begin{aligned} \Gamma_e &= [\Gamma_{11} \ 2\Gamma_{12} \ \Gamma_{22}]^T & 2\Gamma_s &= [2\Gamma_{13} \ 2\Gamma_{23}]^T & \Gamma_t &= \Gamma_{33} \\ \epsilon &= [\varepsilon_{11} \ 2\varepsilon_{12} \ \varepsilon_{22}]^T & \kappa &= [K_{11} \ K_{12} + K_{21} \ K_{22}]^T \\ I_1 &= \begin{bmatrix} 1 & 0 & 0 \\ 0 & 1 & 0 \end{bmatrix}^T & I_2 &= \begin{bmatrix} 0 & 1 & 0 \\ 0 & 0 & 1 \end{bmatrix}^T & e_1 &= \begin{Bmatrix} 1 \\ 0 \end{Bmatrix} & e_2 &= \begin{Bmatrix} 0 \\ 1 \end{Bmatrix} \end{aligned} \quad (13)$$

Now, the strain energy of the plate per unit area (which is the same as the strain energy for the deformation of the normal-line element) can be written as

$$U = \frac{1}{2} \left\langle \begin{Bmatrix} \Gamma_e \\ 2\Gamma_s \\ \Gamma_t \end{Bmatrix}^T \begin{bmatrix} D_e & D_{es} & D_{et} \\ D_{es}^T & D_s & D_{st} \\ D_{et}^T & D_{st}^T & D_t \end{bmatrix} \begin{Bmatrix} \Gamma_e \\ 2\Gamma_s \\ \Gamma_t \end{Bmatrix} \right\rangle \quad (14)$$

where D_e , D_{es} , D_{et} , D_s , D_{st} and D_t are the appropriate partition matrices of the original 3-D 6×6 material matrix. It is noted that the material matrix should be expressed in the global coordinates system x_i and is in general fully populated. However, if it is desired to model laminated composite plates in which each lamina exhibits a monoclinic symmetry about its own mid-plane and is rotated about the local normal to be a layer in the composite laminated plate, then D_{es} and D_{st} will always vanish no matter what the layup angle is. Considering this, we can simplify the strain energy expression to the form

$$2U = \langle \Gamma_e^T D_e \Gamma_e + 2\Gamma_e^T D_{et} \Gamma_t + 2\Gamma_s^T D_s 2\Gamma_s + \Gamma_t^T D_t \Gamma_t \rangle \quad (15)$$

To deal with applied loads, we will at first leave open the existence of a potential energy and develop instead the virtual work of the applied loads. The virtual displacement is taken as the Lagrangean variation of the displacement field, such that

$$\delta \hat{\mathbf{R}} = \overline{\delta q_{B_i}} \mathbf{B}_i + x_3 \delta \mathbf{B}_3 + \delta w_i \mathbf{B}_i + w_j \delta \mathbf{B}_j \quad (16)$$

where the virtual displacement and rotation are defined as

$$\overline{\delta q_{B_i}} = \delta \mathbf{u} \cdot \mathbf{B}_i \quad \delta \mathbf{B}_i = (-\overline{\delta \psi_{B\beta}} \mathbf{B}_\beta \times \mathbf{B}_3 + \overline{\delta \psi_{B_3}} \mathbf{B}_3) \times \mathbf{B}_i \quad (17)$$

Since both the strain and the warping are small, one may safely ignore products of the warping and the loading in the virtual rotation term. Then, the virtual work done by the applied loads $\tau_i \mathbf{B}_i$ at the top surface, $\beta_i \mathbf{B}_i$ at the bottom surface, and body force $\phi_i \mathbf{B}_i$

through the thickness is

$$\begin{aligned} \overline{\delta W} = & (\tau_i + \beta_i + \langle \phi_i \rangle) \overline{\delta q}_{Bi} + \overline{\delta \psi}_{B\alpha} \left[\frac{h}{2} (\tau_\alpha - \beta_\alpha) + \langle x_3 \phi_\alpha \rangle \right] \\ & + \delta (\tau_i w_i^+ + \beta_i w_i^- + \langle \phi_i w_i \rangle) \end{aligned} \quad (18)$$

where τ_i , β_i , and ϕ_i are taken to be independent of the warping functions, $(\)^+ = (\)|_{x_3=\frac{h}{2}}$, and $(\)^- = (\)|_{x_3=-\frac{h}{2}}$. By introducing column matrices $\overline{\delta q}$, $\overline{\delta \psi}$, τ , β , and ϕ , which are formed by stacking the three elements associated with indexed symbols of the same names, one may write the virtual work in a matrix form, so that

$$\overline{\delta W} = \overline{\delta q}^T f + \overline{\delta \psi}^T m + \delta (\tau^T w^+ + \beta^T w^- + \langle \phi^T w \rangle) \quad (19)$$

where

$$\begin{aligned} f &= \tau + \beta + \langle \phi \rangle \\ m &= \left\{ \begin{array}{c} \frac{h}{2} (\tau_1 - \beta_1) + \langle x_3 \phi_1 \rangle \\ \frac{h}{2} (\tau_2 - \beta_2) + \langle x_3 \phi_2 \rangle \\ 0 \end{array} \right\} \end{aligned} \quad (20)$$

The complete statement of the problem can now be presented in terms of the principle of virtual work, such that

$$\delta U - \overline{\delta W} = 0 \quad (21)$$

This is the variational statement of the original 3-D geometrically nonlinear problem with $\overline{\delta q}$, $\overline{\delta \psi}$, and δw as the variables. For construction of a reduced model with $\overline{\delta q}$ and $\overline{\delta \psi}$ as the variables, we consider them as fixed and only the warping function could be varied. In spite of the possibility of accounting for nonconservative forces in the above variational statement, we can assume the dependence of τ , β , and ϕ on the warping functions are negligible to render the problem governing the warping functions conservative. Thus, one can pose the problem that governs the warping as the minimization of a total potential functional

$$\delta \Pi = 0 \quad \text{with} \quad \Pi = U - \tau^T w^+ - \beta^T w^- - \langle \phi^T w \rangle \quad (22)$$

in which only the warping functions are varied, subject to the constraints Eq. (6). Up to this point, this is simply an alternative formulation of the original 3-D elasticity problem. If we attempt to solve this problem directly, we will meet the same difficulty as solving any full 3-D elasticity problem. Fortunately, as shown below, VAM can be used to calculate the 3-D unknown warping functions asymptotically.

Dimensional Reduction

To rigorously reduce the original 3-D problem to a 2-D plate problem, one must attempt to reproduce the energy stored in the 3-D structure in a 2-D formulation. This dimensional reduction can only be done approximately, and one way to do it is by taking advantage of the smallness of h/l . As mentioned previously, although the reduced models based on *ad hoc* kinematic assumptions regularly appear in the literature, there is no rigorous justification for such assumptions. Rather, in this work, VAM will be used to mathematically perform a dimensional reduction of the 3-D problem to a series of 2-D models. To proceed by this method, one has to assess and keep track of the order of all the quantities in the formulation. Following Sutyrin (1997), the quantities of interest have the following orders:

$$\begin{aligned} \epsilon &\sim h\kappa \sim \delta & f_3 &\sim \mu(h/l)^2\delta \\ f_\alpha &\sim \mu(h/l)\delta & m_\alpha &\sim \mu h(h/l)\delta \end{aligned} \quad (23)$$

where δ is the order of the maximum strain in the plate and μ is the order of the material constants (all of which are assumed to be of the same order).

Having assessed the orders of quantities of interest, we can use VAM to mathematically perform the dimensional reduction. Instead of following the scheme used in the previous work by the writer and his co-workers (Yu *et al.* (2002), Yu *et al.* (2003), and Yu and Hodges (2004)), here we choose to follow the original application of VAM in Berdichevsky (1979). The total potential energy can be expressed explicitly in terms of the 2-D variables and warping functions as:

$$\begin{aligned} 2\Pi &= \langle (\epsilon + x_3\kappa + I_\alpha w_{\parallel,\alpha})^T D_e (\epsilon + x_3\kappa + I_\beta w_{\parallel,\beta}) \rangle \\ &+ 2 \langle (\epsilon + x_3\kappa + I_\alpha w_{\parallel,\alpha})^T D_{et} w'_3 + w'_3 D_t w'_3 \rangle \\ &+ \langle (w'_\parallel + e_\alpha w_{3,\alpha})^T D_s (w'_\parallel + e_\beta w_{3,\beta}) - 2\phi^T w \rangle \\ &- 2\tau^T w^+ - 2\beta^T w^- \end{aligned} \quad (24)$$

According to the asymptotical analysis and Eq. (23), we know

$$\begin{aligned} (I_\alpha w_{\parallel,\alpha})^T D_e I_\beta w_{\parallel,\beta} &\ll w_\parallel^T D_s w'_\parallel \\ (e_\alpha w_{3,\alpha})^T D_s e_\beta w_{3,\beta} &\ll w_3^T D_t w'_3 \\ \tau_3 w_3^+ \sim \beta_3 w_3^- &\sim \phi_3 w_3 \ll (\epsilon + x_3\kappa)^T D_{et} w'_3 \end{aligned} \quad (25)$$

The orders of $(I_\alpha w_{\parallel,\alpha})^T D_{et} w'_3$ and $w_\parallel^T D_s e_\alpha w_{3,\alpha}$ are unknown at this point, and we will discard them first as suggested in Berdichevsky (1979). Then the energy functional can be simplified

by retaining only the leading terms so that:

$$\begin{aligned}
2\Pi^* &= \langle (\epsilon + x_3\kappa)^T D_e(\epsilon + x_3\kappa) + 2(\epsilon + x_3\kappa)^T D_e I_\alpha w_{\parallel,\alpha} \rangle \\
&+ 2 \langle (\epsilon + x_3\kappa)^T D_{et} w'_3 + w'_3 D_t w'_3 + w_{\parallel}^T D_s w'_{\parallel} \rangle \\
&- 2 \langle \phi_{\parallel}^T w_{\parallel} \rangle - 2\tau_{\parallel}^T w_{\parallel}^+ - 2\beta_{\parallel}^T w_{\parallel}^-
\end{aligned} \tag{26}$$

In the above functional, w_3 is decoupled from w_{\parallel} and can be solved separately, such that

$$w_3 = (D_{\perp} + L_3)\mathcal{E} \tag{27}$$

where

$$\begin{aligned}
D_{\perp} &= [D_{\perp 1} \ D_{\perp 2}] \quad \mathcal{E} = [\epsilon \ \kappa]^T \quad L_3 \mathcal{E} = c_3/h \\
D'_{\perp 1} &= -D_{et}^T/D_t \quad D'_{\perp 2} = -x_3 D_{et}^T/D_t \quad \langle D_{\perp \alpha} \rangle = 0
\end{aligned} \tag{28}$$

Note that inter-lamina continuity of $D_{\perp \alpha}$ must be maintained due to the continuity of warping functions to produce a continuous displacement field. L_3 contains six constants to be determined later. We know from Eq. (27) that $w_3 \sim h\delta$, which means the previously discarded terms $(I_\alpha w_{\parallel,\alpha})^T D_{et} w'_3$ and $w_{\parallel}^T D_s e_\alpha w_{3,\alpha}$ are of the same order as $(\epsilon + x_3\kappa)^T D_e I_\alpha w_{\parallel,\alpha}$ and they should be retained for the calculation of w_{\parallel} . Whether they should be kept for the calculation of w_3 can only be ascertained after we have found w_{\parallel} . The energy functional including the leading terms to solve w_{\parallel} is:

$$\begin{aligned}
2\Pi^* &= \langle (\epsilon + x_3\kappa)^T D_{\parallel}(\epsilon + x_3\kappa) + 2(\epsilon + x_3\kappa)^T D_{\parallel} I_\alpha w_{\parallel,\alpha} \rangle \\
&+ \langle (w'_{\parallel} + e_\alpha w_{3,\alpha})^T D_s (w'_{\parallel} + e_\alpha w_{3,\alpha}) - 2\phi_{\parallel}^T w_{\parallel} \rangle \\
&- 2\tau_{\parallel}^T w_{\parallel}^+ - 2\beta_{\parallel}^T w_{\parallel}^- - 2 \langle \phi_3 w_3 \rangle - 2\tau_3 w_3^+ - 2\beta_3 w_3^-
\end{aligned} \tag{29}$$

where w_3 is known from Eq. (27), and $D_{\parallel} = D_e - D_{et} D_{et}^T/D_t$. To carry out the variations of the functional, one should be aware that w_{\parallel} may be different functions for each layer. The continuity conditions on the interfaces can be derived following calculus of variations as:

$$[w_{\parallel}] = 0 \quad [D_s(w'_{\parallel} + e_\alpha w_{3,\alpha})] = 0 \quad \text{on} \quad \Omega_i \tag{30}$$

where Ω_i denote the interfaces between the i th layer and $i + 1$ th layer for $i = 1 \dots N - 1$ with N as the total number of layers and the bracket $[\cdot]$ denotes the jump of the enclosed

argument on the interface. The Euler equations and the remaining conditions are:

$$\begin{aligned}
(D_s w'_\parallel + D_s e_\alpha w_{3,\alpha})' &= C'_\alpha \mathcal{E}_{,\alpha} + g' + \lambda_\parallel \\
(D_s w'_\parallel + D_s e_\alpha w_{3,\alpha})^+ &= \tau_\parallel \\
(D_s w'_\parallel + D_s e_\alpha w_{3,\alpha})^- &= -\beta_\parallel
\end{aligned} \tag{31}$$

where $C'_\alpha = -I_\alpha^T [D_\parallel \ x_3 D_\parallel]$, $g' = -\phi_\parallel$, and λ_\parallel are Lagrange multipliers to enforce the constraints applied on the warping functions, Eq. (6). The inter-lamina continuity on C_α and g are maintained to take advantage of the second condition in Eq. (30). We also let $\langle C_\parallel \rangle = 0$ and $\langle g \rangle = 0$ to eliminate all the integration constants for convenience of future calculation. Integration by parts with respect to the in-plane coordinates is used here and hereafter, whenever it is convenient for the derivation, since the goal is to obtain an interior solution for the plate without consideration of edge effects.

Solving the equations in Eqs. (31) along with (6), one obtains the following warping functions

$$w_\parallel = (\bar{C}_\alpha + L_\alpha - x_3 e_\alpha L_3) \mathcal{E}_{,\alpha} + \bar{g} \tag{32}$$

with

$$\begin{aligned}
\bar{C}'_\alpha &= D_s^{-1} C_\alpha^* \quad \langle \bar{C}_\alpha \rangle = 0 \quad \bar{g}' = D_s^{-1} g^* \quad \langle \bar{g} \rangle = 0 \quad L_\alpha \mathcal{E}_{,\alpha} = c_\parallel / h \\
C_\alpha^* &= C_\alpha + \frac{x_3}{h} C_\alpha^\mp - \frac{1}{2} C_\alpha^\pm - D_s e_\alpha D_\perp \\
g^* &= g + \frac{x_3}{h} g^\mp - \frac{1}{2} g^\pm + \left(\frac{x_3}{h} + \frac{1}{2} \right) \tau_\parallel + \left(\frac{x_3}{h} - \frac{1}{2} \right) \beta_\parallel
\end{aligned} \tag{33}$$

where the notation $()^\pm = ()^+ + ()^-$ and $()^\mp = ()^- - ()^+$. The order of w_\parallel is $(h/l)\delta$, which means $(I_\alpha w_{\parallel,\alpha})^T D_{et} w'_3$ and $w_\parallel^T D_s e_\alpha w_{3,\alpha}$ are much smaller than $w'_3 D_t w'_3$ and discarding these two terms will not affect the calculation of w_3 .

Now we have all the information needed to obtain the total energy that is asymptotically correct through the order of $\mu(h/l)^2 \delta^2$ which is sufficient for construction of a Reissner-Mindlin model, viz.,

$$2\Pi_1 = \mathcal{E}^T A \mathcal{E} + \mathcal{E}_1^T B \mathcal{E}_{,1} + 2\mathcal{E}_{,1}^T C \mathcal{E}_{,2} + \mathcal{E}_2^T D \mathcal{E}_{,2} - 2\mathcal{E}^T F \tag{34}$$

where

$$\begin{aligned}
B &= \left\langle D_{s_{11}} D_{\perp}^T D_{\perp} + \bar{C}_1^T C'_1 + C_1^{*T} e_1 D_{\perp} \right\rangle - 2L_1^T C_1^{\mp} + 2L_3^T e_1^T E_1 \\
C &= \left\langle D_{s_{12}} D_{\perp}^T D_{\perp} + \frac{1}{2} (\bar{C}_1^T C'_2 + C_1'^T \bar{C}_2 + C_1^{*T} e_2 D_{\perp} + D_{\perp}^T e_1^T C_2^*) \right\rangle \\
&\quad - L_1^T C_2^{\mp} - C_1^{\mp T} L_2 + L_3^T e_1^T E_2 + E_1^T e_2 L_3 \\
D &= \left\langle D_{s_{22}} D_{\perp}^T D_{\perp} + \bar{C}_2^T C'_2 + C_2^{*T} e_2 D_{\perp} \right\rangle - 2L_2^T C_2^{\mp} + 2L_3^T e_2^T E_2 \\
F &= \tau_3 D_{\perp}^{+T} + \beta_3 D_{\perp}^{-T} + \langle \phi_3 D_{\perp}^T \rangle + L_3^T (\tau_3 + \beta_3 + \langle \phi_3 \rangle) \\
&\quad + \frac{1}{2} \left\langle \left\langle D_{\perp}^T e_{\alpha}^T g_{,\alpha}^* + C_{\alpha}^{\prime T} \bar{g}_{,\alpha} - \bar{C}_{\alpha}^T \phi_{\parallel,\alpha} \right\rangle - \bar{C}_{\alpha}^{+T} \tau_{\parallel,\alpha} - \bar{C}_{\alpha}^{-T} \beta_{\parallel,\alpha} \right\rangle \\
&\quad - L_{\alpha}^T (\tau_{\parallel,\alpha} + \beta_{\parallel,\alpha} + g_{,\alpha}^{\mp}) + \frac{h}{2} L_3^T e_{\alpha}^T (\tau_{\parallel,\alpha} - \beta_{\parallel,\alpha} - g_{,\alpha}^{\pm}) \\
A &= \begin{bmatrix} \langle D_{\parallel} \rangle & \langle x_3 D_{\parallel} \rangle \\ \langle x_3 D_{\parallel} \rangle & \langle x_3^2 D_{\parallel} \rangle \end{bmatrix} \quad E_{\alpha} = I_{\alpha} [\langle x_3 D_{\parallel} \rangle \quad \langle x_3^2 D_{\parallel} \rangle] \tag{35}
\end{aligned}$$

Eq. (34) is an energy functional expressed in terms of 2-D variables which can approximate the original 3-D energy asymptotically. It is noted that quadratic terms associated with the applied loads are dropped because they cannot be varied in the 2-D plate model.

Transforming Into Reissner-Mindlin Model

Although Eq. (34) is asymptotically correct through the second order and straightforward use of this strain energy is possible, it involves more complicated boundary conditions than necessary since it contains derivatives of the generalized strain measures. To obtain an energy functional that is of practical use, one can transform Eq. (34) into a Reissner-Mindlin model. In a Reissner-Mindlin model, there are two additional degrees of freedom, which are the transverse shear strains incorporated into the rotation of transverse normal. We introduce another triad \mathbf{B}_i^* for the deformed plate, so that the definition of 2-D strains becomes

$$\begin{aligned}
\mathbf{R}_{,\alpha} &= \mathbf{B}_{\alpha}^* + \varepsilon_{\alpha\beta}^* \mathbf{B}_{\beta}^* + 2\gamma_{\alpha 3} \mathbf{B}_3^* \\
\mathbf{B}_{i,\alpha}^* &= (-K_{\alpha\beta}^* \mathbf{B}_{\beta}^* \times \mathbf{B}_3^* + K_{\alpha 3}^* \mathbf{B}_3^*) \times \mathbf{B}_i^* \tag{36}
\end{aligned}$$

where the transverse shear strains are $\gamma = [2\gamma_{13} \quad 2\gamma_{23}]^T$. Since \mathbf{B}_i^* is uniquely determined by \mathbf{B}_i and γ , one can derive the following kinematic identity between the strains measures \mathcal{R} of Reissner-Mindlin plate and \mathcal{E}

$$\mathcal{E} = \mathcal{R} - \mathcal{D}_{\alpha} \gamma_{,\alpha} \tag{37}$$

where

$$\begin{aligned}
\mathcal{D}_1 &= \begin{bmatrix} 0 & 0 & 0 & 1 & 0 & 0 \\ 0 & 0 & 0 & 0 & 1 & 0 \end{bmatrix}^T \\
\mathcal{D}_2 &= \begin{bmatrix} 0 & 0 & 0 & 0 & 1 & 0 \\ 0 & 0 & 0 & 0 & 0 & 1 \end{bmatrix}^T \\
\mathcal{R} &= [\varepsilon_{11}^* \quad 2\varepsilon_{12}^* \quad \varepsilon_{22}^* \quad K_{11}^* \quad K_{12}^* + K_{21}^* \quad K_{22}^*]^T
\end{aligned} \tag{38}$$

Now one can express the strain energy, asymptotically correct to the second order, in terms of strains of the Reissner-Mindlin model as

$$\begin{aligned}
2\Pi_1 &= \mathcal{R}^T A \mathcal{R} - 2\mathcal{R}^T A \mathcal{D}_1 \gamma_{,1} - 2\mathcal{R}^T A \mathcal{D}_2 \gamma_{,2} \\
&\quad + \mathcal{R}_{,1}^T B \mathcal{R}_{,1} + 2\mathcal{R}_{,1}^T C \mathcal{R}_{,2} + \mathcal{R}_{,2}^T D \mathcal{R}_{,2} - 2\mathcal{R}^T F
\end{aligned} \tag{39}$$

The generalized Reissner-Mindlin model is of the form

$$2\Pi_{\mathcal{R}} = \mathcal{R}^T A \mathcal{R} + \gamma^T G \gamma - 2\mathcal{R}^T F_{\mathcal{R}} - 2\gamma^T F_{\gamma} \tag{40}$$

To find an equivalent Reissner-Mindlin model Eq. (40) for Eq. (39), one has to eliminate all partial derivatives of the strain. Here equilibrium equations are used to achieve this purpose. From the two equilibrium equations balancing bending moments, one can obtain the following formula

$$G\gamma - F_{\gamma} = \mathcal{D}_{\alpha}^T A \mathcal{R}_{,\alpha} + \begin{Bmatrix} m_1 \\ m_2 \end{Bmatrix} \tag{41}$$

where $F_{\mathcal{R},\alpha}$ is dropped because they are high order terms. Substituting Eq. (41) into Eq. (39), one can show that $F_{\mathcal{R}} = F$ and $F_{\gamma} = 0$. Finally one can rewrite Eq. (39) as

$$2\Pi_1 = \mathcal{R}^T A \mathcal{R} + \gamma^T G \gamma - 2\mathcal{R}^T F + U^* \tag{42}$$

where

$$U^* = \mathcal{R}_{,1}^T \bar{B} \mathcal{R}_{,1} + 2\mathcal{R}_{,1}^T \bar{C} \mathcal{R}_{,2} + \mathcal{R}_{,2}^T \bar{D} \mathcal{R}_{,2} \tag{43}$$

and

$$\begin{aligned}
\bar{B} &= B + A \mathcal{D}_1 G^{-1} \mathcal{D}_1^T A \\
\bar{C} &= C + A \mathcal{D}_1 G^{-1} \mathcal{D}_2^T A \\
\bar{D} &= D + A \mathcal{D}_2 G^{-1} \mathcal{D}_2^T A
\end{aligned} \tag{44}$$

If we can drive U^* to be zero for any \mathcal{R} , then we have found an asymptotically correct Reissner-Mindlin plate model. For general anisotropic plates, this term will not be zero; but we can minimize the error to obtain a Reissner-Mindlin model that is as close to asymptotical correctness as possible. The accuracy of the Reissner-Mindlin model depends on how close to zero one can drive this term. In other words, one needs to seek an optimal set of the 33 unknowns (G contains 3 unknowns, L_3 contains 6 unknowns, and L_α contain 24 unknowns) so that the value of the quadratic form in Eq. (43) is as close to be zero as possible for arbitrary generalized strain measures. Previously, we let the distinct 78 terms in the symmetric 12×12 coefficient matrix equal to zeros to formulate 78 equations. It is a linear system with 33 unknowns. Then we used the least square technique to solve the overdetermined system for the constants as done in Yu *et al.* (2002). Mathematically, it requires us to minimize the maximum absolute of the eigenvalues of the 12×12 coefficient matrix. Such a minimization problem can be written as a semi-definite programming (SDP) problem, Toh *et al.* (1999). The derivation requires some knowledge of advanced matrix analysis like Schur complement theorem. Therefore, the present work will use SDP to carry out the minimization of loss of energy. After driving of U^* to be close to zero, we found the “best”, from the asymptotic point of view, Reissner-Mindlin model to be used for 2-D plate analysis.

$$2\Pi_{\mathcal{R}} = \mathcal{R}^T A \mathcal{R} + \gamma^T G \gamma - 2R^T F \quad (45)$$

with A , G , F capturing the material and geometric information eliminated in the reduced 2-D plate analysis. It is worthy to emphasize that although the 2-D constitutive model is constructed in a way dramatically different from traditional Reissner-Mindlin models, the plate analysis remains the same including the governing equations and essential and natural boundary conditions as long as the strain measures are defined equivalently as in Eqs. (36).

Recovery Relations

From the above, we have obtained a Reissner-Mindlin model for composite plates which is as close as possible to being asymptotically correct in the sense of matching the total energy. One can use this model to carry out various analyses (for example, static, dynamic, buckling, and aeroelastic) for composite plates. In many applications, however, while it is necessary to accurately calculate the 2-D displacement field of composite plates, this is not sufficient. Ultimately, the fidelity of a reduced-order model such as this depends on how well it can predict the 3-D results in the original 3-D structure. Hence recovery relations should be provided to complete the theory so that the results can be compared with those of the original 3-D model. By recovery relations, then, we mean expressions for 3-D displacement, strain, and stress fields in terms of 2-D quantities and x_3 .

For an energy that is asymptotically correct through the second order, we can recover the 3-D displacement, strain, and stress fields only through the first order in a strict sense of asymptotical correctness. Using Eqs. (1), (3), and (4), one can recover the 3-D displacement field through the first order as

$$U_i = u_i + x_3 C_{3i} + C_{ji} w_j \quad (46)$$

where U_i , u_i are the 3-D displacements and plate displacements, respectively, expressed in \mathbf{b}_i . And from Eq. (12), one can recover the 3-D strain field through the first order as

$$\Gamma_e = \epsilon + x_3 \kappa \quad 2\Gamma_s = w'_{\parallel} + e_{\alpha} w_{3,\alpha} \quad \Gamma_t = w'_3 \quad (47)$$

One can use the 3-D constitutive law to obtain 3-D stresses σ_{ij} . Since we have obtained an optimum shear stiffness matrix G , the recovered 3-D results through the first order are better than CLT and conventional first-order shear deformation theory (FOSDT). However, according to the present approach, the transverse normal stress (σ_{33}) is a second-order quantity and not available in the first approximation. Despite that it is usually much smaller than other components, σ_{33} is a very critical component for some failures such as debonding or delamination. In order to obtain a reasonable recovery for the transverse normal stress, VAM needs to be applied one more time to find the warping functions of the order of $(h/l)^2 \delta$. Using the same procedure listed in previous section, the second-order warping function y_3 can be obtained through the following equations

$$\begin{aligned} (D_t y'_3 + D_{et}^T I_{\alpha} w_{\parallel, \alpha})' + e_{\beta}^T D_s (w'_{\parallel} + e_{\alpha} w_{3, \alpha})_{, \beta} + \phi_3 &= \lambda_3 \\ (D_t y'_3 + D_{et}^T I_{\alpha} w_{\parallel, \alpha})^+ &= \tau_3 \\ (D_t y'_3 + D_{et}^T I_{\alpha} w_{\parallel, \alpha})^- &= -\beta_3 \\ [w_3] = 0 \quad [D_t y'_3 + D_{et}^T I_{\alpha} w_{\parallel, \alpha}] &= 0 \quad \text{on } \Omega_i \end{aligned} \quad (48)$$

where λ_3 is the Lagrange multiplier to enforce the constraint $\langle y_3 \rangle = 0$, which is a convenient choice in comparison to Eq. (6). We have obtained an energy asymptotical correct up to the order of $\mu(h/l)^4 \delta^2$ by finding y_3 . Such an energy is way too complex to be used in practice. Therefore, we still use the previous Reissner-Mindlin model to carry out the 2-D plate analysis and consider the 2-D variables as an approximation to those calculated by the fourth-order energy.

Finally, we can write the 3-D recovery relations for displacement through the second order as

$$U_i = u_i + x_3 C_{3i} + C_{ji} w_j + C_{3i} y_3 \quad (49)$$

and the strains through the second order as

$$\Gamma_e = \epsilon + x_3\kappa + I_\alpha w_{\parallel,\alpha} \quad 2\Gamma_s = w'_{\parallel} + e_\alpha w_{3,\alpha} \quad \Gamma_t = w'_3 + y'_3 \quad (50)$$

Again the stresses through the second order can be obtained from use of the 3-D material law, such that

$$\begin{aligned} \sigma_e &\equiv [\sigma_{11} \ \sigma_{12} \ \sigma_{22}]^T = D_{\parallel}(\epsilon + x_3\kappa) + D_{et}y'_3 + D_e I_\alpha w_{\parallel,\alpha} \\ \sigma_s &\equiv [\sigma_{13} \ \sigma_{23}]^T = D_s(w'_{\parallel} + e_\alpha w_{3,\alpha}) \\ \sigma_t &\equiv \sigma_{33} = D_{et}^T I_\alpha w_{\parallel,\alpha} + D_t y'_3 \end{aligned} \quad (51)$$

Before demonstrating the accuracy of the present theory using numerical examples, it is interesting to check the behavior of recovered fields. It is obvious that 3-D displacement fields recovered using Eq. (49) is continuous on the interface of difference layers because the warping functions are continuous on the interfaces. One can also conclude that the recovered 3-D transverse shear and normal stresses from Eq. (51) are also continuous due to the continuous conditions in Eqs. (30) and (48). Furthermore, these components, σ_{i3} , exactly satisfy the traction boundary conditions on the top and bottom surfaces because such conditions are directly utilized to find the solution, as shown in Eqs. (31) and (48). It is of interest to check whether the recovered 3-D stresses satisfy the 3-D equilibrium equations. Here we use the static equilibrium from the 3-D elasticity theory:

$$\sigma_{ij,j} + \phi_i = 0 \quad (52)$$

Plugging the recovered stresses in Eqs. (51) into the above equilibrium equations and dropping terms higher than the second order, one obtains

$$\begin{aligned} [D_s(w'_{\parallel} + e_\alpha w_{3,\alpha})]' + I_\alpha^T D_{\parallel}(\epsilon_{,\alpha} + x_3\kappa_{,\alpha}) + \phi_{\parallel} &= 0 \\ (D_t y'_3 + D_{et}^T I_\alpha w_{\parallel,\alpha})' + e_\beta^T D_s(w'_{\parallel} + e_\alpha w_{3,\alpha})_{,\beta} + \phi_3 &= 0 \end{aligned} \quad (53)$$

In view of the Euler equations in Eqs. (31) and (48), if λ_{\parallel} and λ_3 vanish, Eqs. (53) will be automatically satisfied, which means the recovered stresses can satisfy the 3-D equilibrium asymptotically up to the second order. Integrating Euler equation for w_{\parallel} through the thickness, we get

$$I_\alpha [\langle D_{\parallel} \rangle \ \langle x_3 D_{\parallel} \rangle]^T \mathcal{E}_{,\alpha} + f_{\parallel} = h\lambda_{\parallel} \quad (54)$$

Comparing it with the 2-D equilibrium equations derived from the Reissner-Mindlin model

in Eq. (45), such as the linearized first two equations in Eqs. (60) of Hodges *et al.* (1993), one can show that λ_{\parallel} indeed vanish because the membrane stress resultants are defined as:

$$[N_{11} \ N_{12} \ N_{22}]^T = [\langle D_{\parallel} \rangle \ \langle x_3 D_{\parallel} \rangle]^T \mathcal{E} \quad (55)$$

Therefore, we have proved that the first two 3-D equilibrium equations are satisfied asymptotically up to the second order. Similarly, we can integrate the Euler equation for y_3 to obtain

$$e_{\beta}^T \langle D_s(w'_{\parallel} + e_{\alpha} w_{3,\alpha}) \rangle_{,\beta} + f_3 = h\lambda_3 \quad (56)$$

Only if the transverse shear stress resultants are defined as

$$[Q_1 \ Q_2]^T = \langle D_s(w'_{\parallel} + e_{\alpha} w_{3,\alpha}) \rangle = \langle \sigma_s \rangle \quad (57)$$

will λ_3 vanish due to the third equation of the 2-D equilibrium equation. However, the transverse shear stress resultants are defined directly using Eq. (45), and we have no direct means to establish Eq. (57). Nevertheless, one can reasonably argue that Eq. (57) should be satisfied approximately, not necessary asymptotically, because Eq. (45) is the “best” representation of the original 3-D energy due to σ_e and σ_s in a Reissner-Mindlin model. Then we can safely state that the third 3-D equilibrium equation is satisfied in the sense of minimizing the loss of energy between 3-D energy and the Reissner-Mindlin model.

From above, we have shown analytically that: (a) the recovered 3-D displacements and stresses satisfy the both displacement and traction continuity on the interfaces; (b) the recovered stresses satisfy traction conditions on the top and bottom surfaces; and (c) the recovered 3-D stresses satisfy the first two equations of 3-D equilibrium asymptotically up to the second order and the third equation in the sense of minimal energy loss in a Reissner-Mindlin model. A complete set of such features are not found in the literature on equivalent single-layer models and most of the higher order layerwise models for composite plates.

Numerical Examples

In this section we use a few simple examples to demonstrate the accuracy of the developed theory. The plates we are going to study are made with composite material with the following properties

$$\begin{aligned} E_L &= 25 \times 10^6 \text{ psi} & E_T &= 10^6 \text{ psi} \\ G_{LT} &= 0.5 \times 10^6 \text{ psi} & G_{TT} &= 0.2 \times 10^6 \text{ psi} \\ \nu_{LT} &= \nu_{TT} = 0.25 \end{aligned}$$

where L denotes the direction parallel to the fibers and T the transverse direction. The test problem is a plate with width $L = 4$ in. along x_1 (the “lateral” direction) and infinite length in the x_2 direction (the “longitudinal” direction). The thickness of the plate is 1 in., so that the aspect ratio $L/h = 4$. The plate is simply supported and subjected to a sinusoidal pressure of the form

$$\tau_3 = \beta_3 = \frac{p_0}{2} \sin\left(\frac{\pi x_1}{L}\right) \quad (58)$$

with $\tau_\alpha = \beta_\alpha = 0$. A geometrically linear theory is used in order to compare the results with the available exact solution in Pagano (1970).

First, we investigate a laminated composite plate with lay-up $[15^\circ / -15^\circ]$. The recovered stresses normalized by p_0 are plotted in Figs. 2 – 7, where the solid line represents the results from the exact solution of Pagano (1970), dots from the present theory, dashed line from FOSDT, and long-dash/short-dash line from CLT. Note that, because the 2-D variables are either sine or cosine functions of x_1 , $\sigma_{\alpha\beta}$ and σ_{33} are plotted for the position $x_1 = L/2$, and $\sigma_{\alpha 3}$ are plotted for the position $x_1 = 0$ or $x_1 = L$. From the plots, one can observe that the present theory has an excellent agreement with the 3-D exact solution and produces much better results than CLT and FOSDT, especially for the transverse shear and transverse normal stresses. From the plots, one can also observe that the continuity conditions on the interface and traction conditions on the bottom and top surfaces are satisfied exactly.

Next, we take another composite laminate with lay-up $[30^\circ / -30^\circ / -30^\circ / 30^\circ]$. The results are shown in Figs. 8 – 13. The power of present theory is clearly exemplified by the excellent agreement with exact 3-D solutions. Indeed, even though there are more layers in this example, the agreement is still excellent. Recall that the recovery relations use results from a standard Reissner-Mindlin plate model. The large number of degrees of freedom in the layer-wise models depends on the number of layers and is unnecessary to achieve the level of accuracy shown here.

Lastly, we study a more realistic example with 20 layers with the stacking sequence as $[30^\circ / -30^\circ / -30^\circ / 30^\circ]_5$. The stresses are shown in Figs. 14 – 19. As one can observe from the results, even for this case, the present theory agrees with exact solution very well. This clearly proves that one can use the present theory to model laminated plates confidently to get great accuracy with much less computational effort.

For all the simple cylindrical bending problems we have tested, the results of the present theory are almost identical to that of Yu *et al.* (2002). However, we believe that present model is more robust and should yield better results for more realistic cases. Such a comparison will require extensive work and is planned for the near future. Furthermore, the present theory has its own academic merit in comparison to that of Yu *et al.* (2002) because it rigorously and consistently introduces the constants from the very beginning while the

previous model introduced the constants as a remedy at the point when it was found out that the minimization problem is too rigid. Hence, the present derivation can be viewed as an analytical justification of Yu *et al.* (2002).

Mathematically, the accuracy of the present theory should be comparable to that of a layer-wise plate theory with assumed in-plane displacements as layer-wise cubic polynomials of the thickness direction and transverse displacement as a layer-wise fourth-order polynomial. The computational cost of the present theory includes both the time of through-the-thickness analysis used by VAPAS and the time of a plate analysis used by a generic 2D plate solver. VAPAS takes a little bit longer than the time used in FOSDT for integration through the thickness. However, one only needs to run VAPAS once for the areas of the plate which has the same through-the-thickness information. The computation time used by VAPAS is almost negligible comparing to the large amount of time used in the plate analysis. Hence, the computational requirement of the present theory is almost the same as FOSDT and much less than layer-wise theories. Moreover, it is not necessary to use integration of the 3-D equilibrium equations through the thickness to get the transverse shear and normal stress results presented herein.

Conclusion

The variational asymptotic method, a powerful mathematical approach, has been used to construct a highly accurate Reissner-Mindlin plate theory for composite laminated plates. The theory is applicable to plates for which each layer is made with a monoclinic material. Although the resulting plate theory is as simple as a single-layer FOSDT, the recovered 3-D displacement, strain, and stress results have excellent accuracy, comparable to that of higher-order, layer-wise plate theories that have many more degrees of freedom. The present paper has built on the writer's previous work in Yu *et al.* (2002) with the following new contributions:

1. The present work allows the maximum freedom (33 constants in total) to seek the optimal Reissner-Mindlin model;
2. The present work adopts the semi-definite programming technique to carry out the optimization;
3. The present work proves the first time that: (a) the recovered 3-D displacements and stresses satisfy the continuity conditions on the interface of different layers; (b) the recovered 3-D stresses satisfy the traction conditions on the bottom and top surfaces; and (c) the recovered 3-D stresses satisfy the first two equilibrium equations asymp-

totically and satisfy the third equation approximately in the sense of minimal energy loss.

Since all the formulas are given in an explicit analytical form, it is easy to implement the present theory using a symbolic manipulator such as Mathematica™ or Maple™. However, for the ultimate goal to use this theory with general 2-D plate solvers, the present theory is incorporated into the computer program VAPAS (variational asymptotic plate and shell analysis). It is a 1-D finite element code which executes very rapidly, enabling this high-fidelity model to be cheaply included in standard plate finite element codes.

Acknowledgements

Technical discussions with Drs. Dewey Hodges and Vitali Volovoi of Georgia Tech regarding the variational asymptotic method, Dr. Kim-Chuan Toh of National University of Singapore and Mr. Zhaosong Lu of Georgia Tech regarding semi-definite programming are greatly appreciated.

References

- Berdichevsky, V. L. (1979). Variational-asymptotic method of constructing a theory of shells. *PMM* 43, 664 – 687.
- Cho, Y. B. and Averill, R. C. (2000). First-order zig-zag sublaminar plate theory and finite element model for laminated composite and sandwich panels. *Composite Structures* 50, 1 – 15.
- Danielson, D. A. (1991). Finite rotation with small strain in beams and plates. In Proceedings of the 2nd Pan American Congress of Applied Mechanics. Valparaiso, Chile. Valparaiso Chile.
- DiSciuva, M. (1985). Development of anisotropic multilayered shear deformable rectangular plate element. *Computers and Structures* 21, 789 – 796.
- Hodges, D. H., Atilgan, A. R. and Danielson, D. A. (1993). A geometrically nonlinear theory of elastic plates. *Journal of Applied Mechanics* 60, 109 – 116.
- Noor, A. K. and Burton, W. S. (1989). Assessment of shear deformation theories for multilayered composite plates. *Applied Mechanics Review* 41, 1 – 13.
- Noor, A. K. and Burton, W. S. (1990). Assessment of computational models for multilayered composite shells. *Applied Mechanics Review* 43.

- Noor, A. K. and Malik, M. (2000). An assessment of five modeling approaches for thermo-mechanical stress analysis of laminated composite panels. *Computational Mechanics* 25, 43–58.
- Pagano, N. J. (1970). Influence of shear coupling in cylindrical bending of anisotropic laminates. *Journal of Composite Materials* 4, 330 – 343.
- Reddy, J. N. (1984). A simple higher-order theory for laminated composite plates. *Journal of Applied Mechanics* 51, 745 – 752.
- Sutyrin, V. G. (1997). Derivation of plate theory accounting asymptotically correct shear deformation. *Journal of Applied Mechanics* 64, 905 – 915.
- Toh, K., Todd, M. and Tutuncu, R. (1999). SDPT3 — a matlab software package for semidefinite programming. *Optimization Methods and Software* 11, 545–581.
- Touratier, M. (1991). An efficient standard plate theory. *International Journal of Engineering Science* 29, 901 – 916.
- Yu, W. and Hodges, D. H. (2004). An asymptotic approach for thermoelastic analysis of laminated composite plates. *Journal of Engineering Mechanics* 130, 531 – 540.
- Yu, W., Hodges, D. H. and Volovoi, V. V. (2002). Asymptotic construction of Reissner-like models for composite plates with accurate strain recovery. *International Journal of Solids and Structures* 39, 5185 – 5203.
- Yu, W., Hodges, D. H. and Volovoi, V. V. (2003). Asymptotically accurate 3-D recovery from Reissner-like composite plate finite elements. *Computers and Structures* 81, 439 – 454.

List of Figure Captions

Figure 1: Schematic of plate deformation

Figure 2: Distribution of σ_{11} vs the thickness coordinate ($[15^\circ / -15^\circ]$) Solid line: exact solution; dots: VAPAS; dashed line: FOSDT; long-dash/short-dash line: CLT.

Figure 3: Distribution of σ_{12} vs the thickness coordinate ($[15^\circ / -15^\circ]$) Solid line: exact solution; dots: VAPAS; dashed line: FOSDT; long-dash/short-dash line: CLT.

Figure 4: Distribution of σ_{22} vs the thickness coordinate ($[15^\circ / -15^\circ]$) Solid line: exact solution; dots: VAPAS; dashed line: FOSDT; long-dash/short-dash line: CLT.

Figure 5: Distribution of σ_{13} vs the thickness coordinate ($[15^\circ / -15^\circ]$) Solid line: exact solution; dots: VAPAS; dashed line: FOSDT; long-dash/short-dash line: CLT.

Figure 6: Distribution of σ_{23} vs the thickness coordinate ($[15^\circ / -15^\circ]$) Solid line: exact solution; dots: VAPAS; dashed line: FOSDT; long-dash/short-dash line: CLT.

Figure 7: Distribution of σ_{33} vs the thickness coordinate ($[15^\circ / -15^\circ]$) Solid line: exact solution; dots: VAPAS; dashed line: FOSDT; long-dash/short-dash line: CLT.

Figure 8: Distribution of σ_{11} vs the thickness coordinate ($[30^\circ / -30^\circ / -30^\circ / 30^\circ]$) Solid line: exact solution; dots: VAPAS; dashed line: FOSDT; long-dash/short-dash line: CLT.

Figure 9: Distribution of σ_{12} vs the thickness coordinate ($[30^\circ / -30^\circ / -30^\circ / 30^\circ]$) Solid line: exact solution; dots: VAPAS; dashed line: FOSDT; long-dash/short-dash line: CLT.

Figure 10: Distribution of σ_{22} vs the thickness coordinate ($[30^\circ / -30^\circ / -30^\circ / 30^\circ]$) Solid line: exact solution; dots: VAPAS; dashed line: FOSDT; long-dash/short-dash line: CLT.

Figure 11: Distribution of σ_{13} vs the thickness coordinate ($[30^\circ / -30^\circ / -30^\circ / 30^\circ]$) Solid line: exact solution; dots: VAPAS; dashed line: FOSDT; long-dash/short-dash line: CLT.

Figure 12: Distribution of σ_{23} vs the thickness coordinate ($[30^\circ / -30^\circ / -30^\circ / 30^\circ]$) Solid line: exact solution; dots: VAPAS; dashed line: FOSDT; long-dash/short-dash line: CLT.

Figure 13: Distribution of σ_{33} vs the thickness coordinate ($[30^\circ / - 30^\circ / - 30^\circ / 30^\circ]$)
Solid line: exact solution; dots: VAPAS; dashed line: FOSDT; long-dash/short-dash line: CLT.

Figure 14: Distribution of σ_{11} vs the thickness coordinate ($[30^\circ / - 30^\circ / - 30^\circ / 30^\circ]_5$)
Solid line: exact solution; dots: VAPAS; dashed line: FOSDT; long-dash/short-dash line: CLT.

Figure 15: Distribution of σ_{12} vs the thickness coordinate ($[30^\circ / - 30^\circ / - 30^\circ / 30^\circ]_5$)
Solid line: exact solution; dots: VAPAS; dashed line: FOSDT; long-dash/short-dash line: CLT.

Figure 16: Distribution of σ_{22} vs the thickness coordinate ($[30^\circ / - 30^\circ / - 30^\circ / 30^\circ]_5$)
Solid line: exact solution; dots: VAPAS; dashed line: FOSDT; long-dash/short-dash line: CLT.

Figure 17: Distribution of σ_{13} vs the thickness coordinate ($[30^\circ / - 30^\circ / - 30^\circ / 30^\circ]_5$)
Solid line: exact solution; dots: VAPAS; dashed line: FOSDT; long-dash/short-dash line: CLT.

Figure 18: Distribution of σ_{23} vs the thickness coordinate ($[30^\circ / - 30^\circ / - 30^\circ / 30^\circ]_5$)
Solid line: exact solution; dots: VAPAS; dashed line: FOSDT; long-dash/short-dash line: CLT.

Figure 19: Distribution of σ_{33} vs the thickness coordinate ($[30^\circ / - 30^\circ / - 30^\circ / 30^\circ]_5$)
Solid line: exact solution; dots: VAPAS; dashed line: FOSDT; long-dash/short-dash line: CLT.

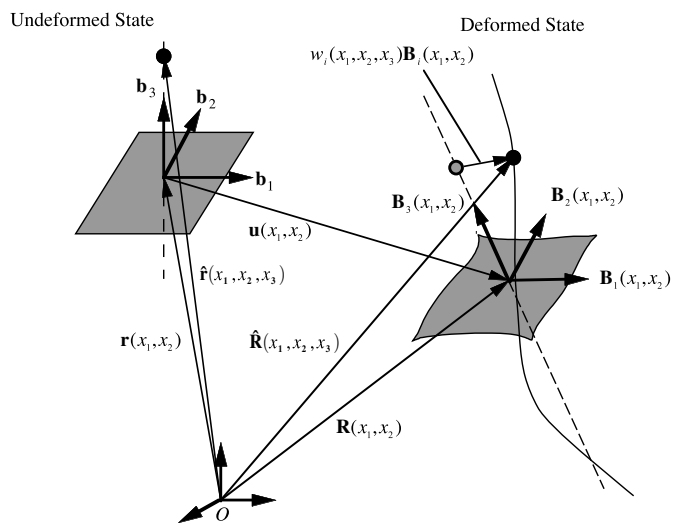


FIGURE 1:

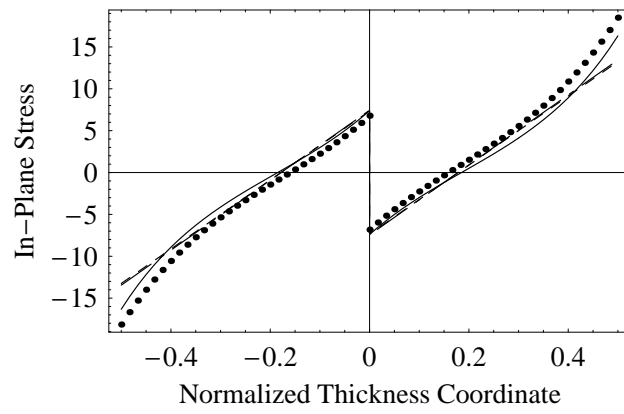


FIGURE 2:

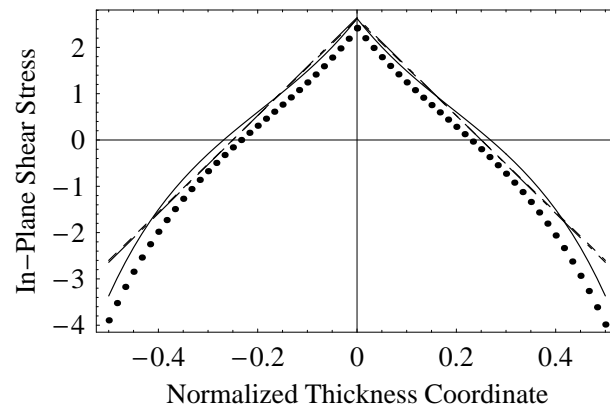


FIGURE 3:

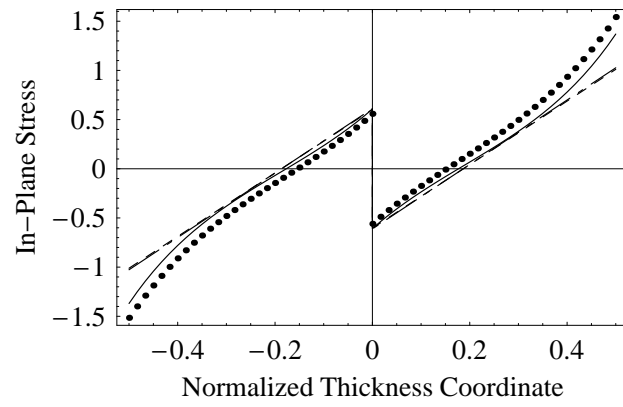


FIGURE 4:

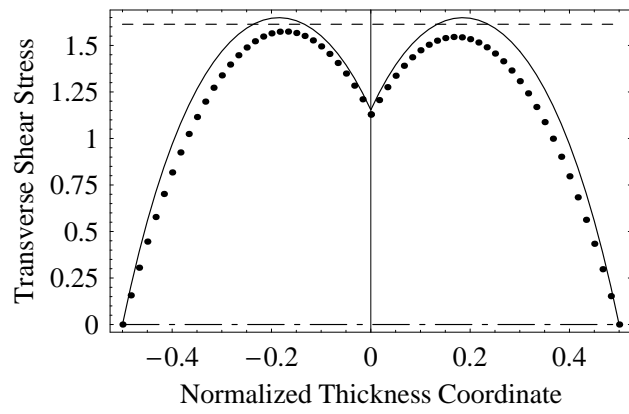


FIGURE 5:

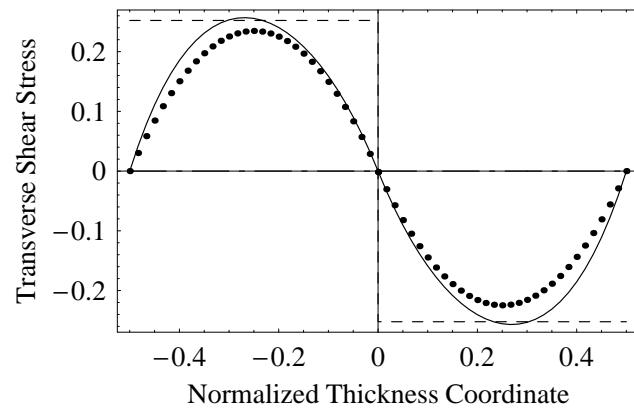


FIGURE 6:

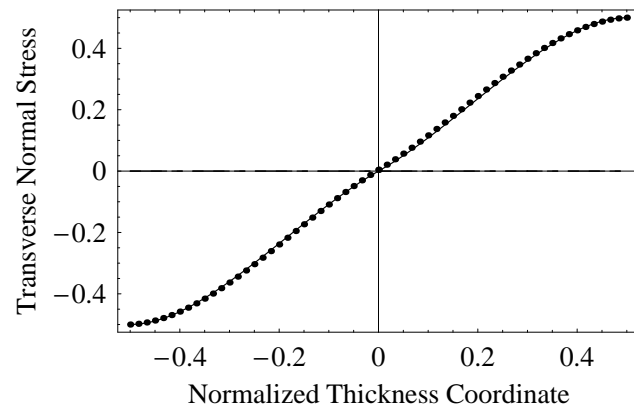


FIGURE 7:

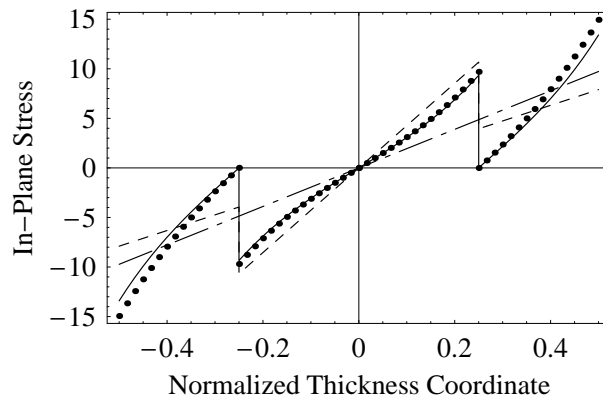


FIGURE 8:

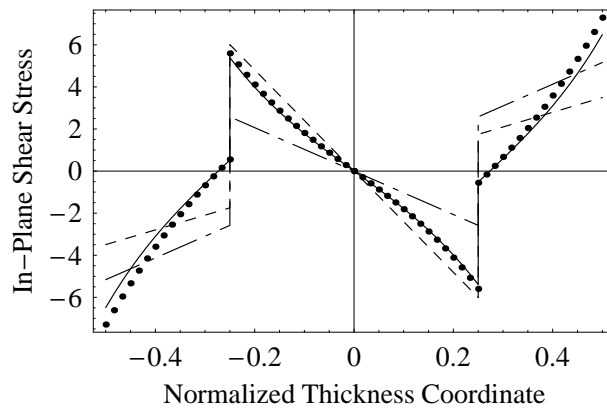


FIGURE 9:

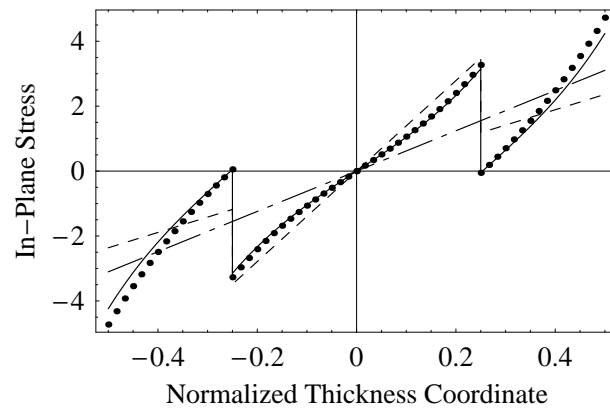


FIGURE 10:

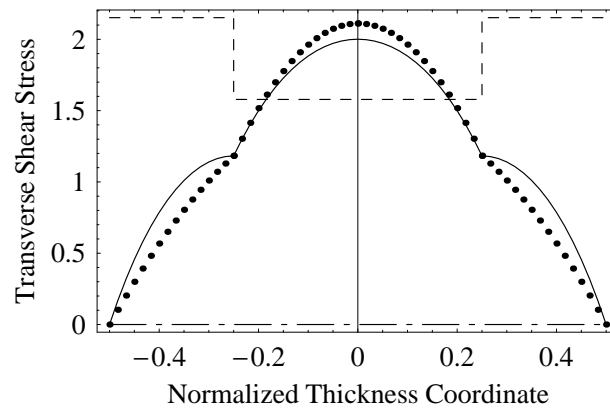


FIGURE 11:

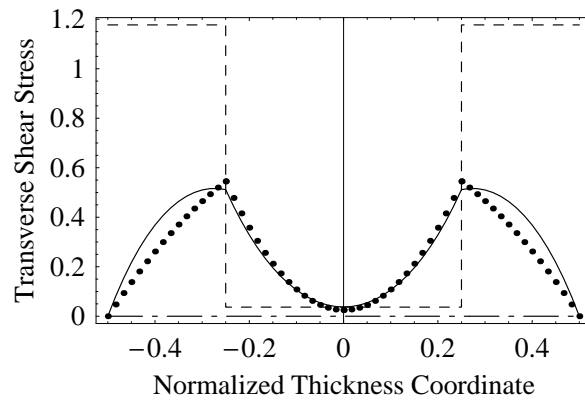


FIGURE 12:

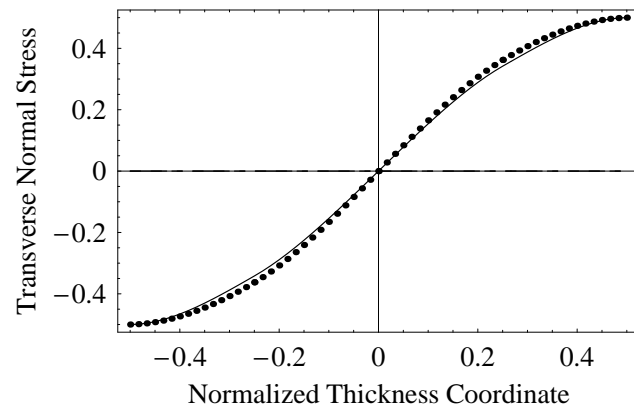


FIGURE 13:

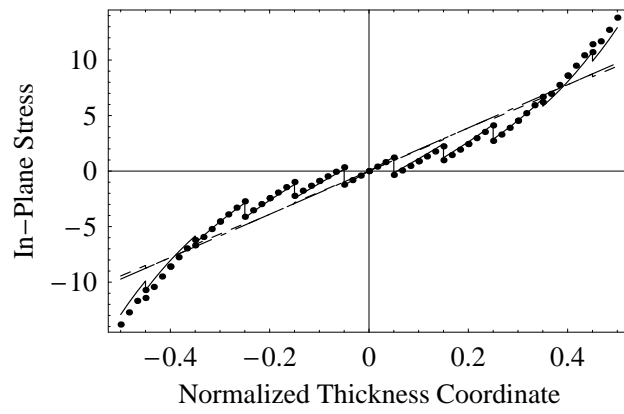


FIGURE 14:

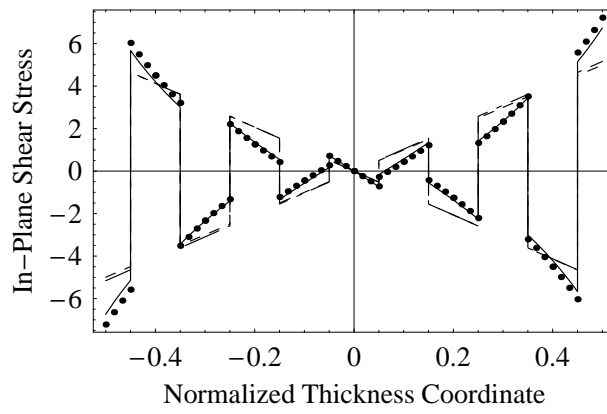


FIGURE 15:

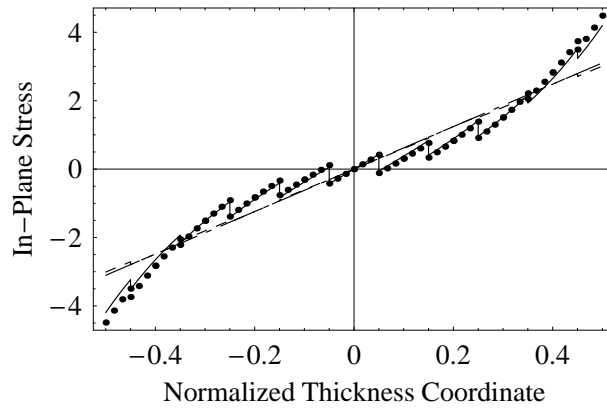


FIGURE 16:

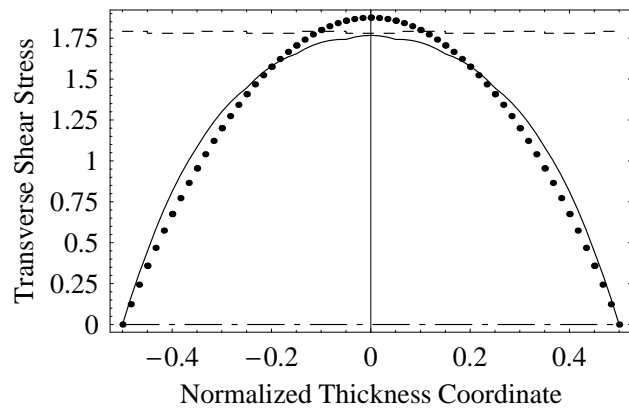


FIGURE 17:

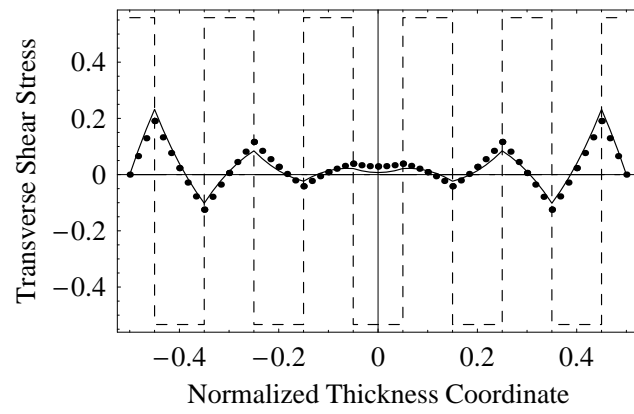


FIGURE 18:

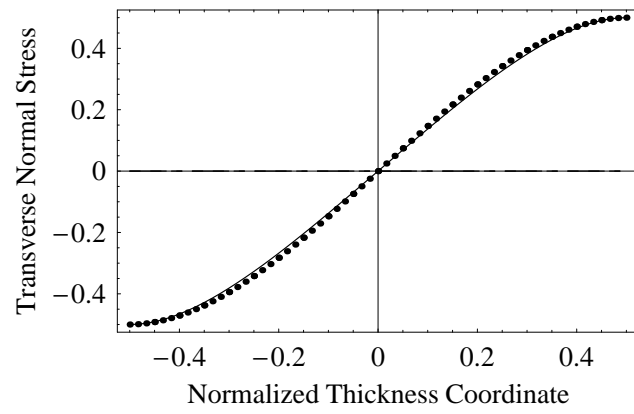


FIGURE 19: